Inverse Power Potentials: Virial Coefficients and a General Equation of State

Richard J. Wheatley

School of Chemistry, University of Nottingham, Nottingham NG7 2RD, U.K.

Received: November 8, 2004; In Final Form: February 8, 2005

Virial coefficients up to the seventh are calculated for pair potentials depending on inverse powers of separation, for inverse powers from 5 to 80. Unlike the limiting (infinite inverse power) hard-sphere potential, some virial coefficients for finite inverse power potentials are found to be negative. This makes resummation of the virial series for general inverse power potentials more difficult than that for hard spheres, and some alternative resummation methods are presented and compared. A general equation of state is proposed for fluids of particles interacting through inverse power pair potentials, for inverse powers greater than about 10. This includes the "molecular" inverse power of 12, for which the current results support and extend the results of previous studies.

I. Background

The inverse power potential

$$E = \epsilon(R/\sigma)^{-n} \tag{1}$$

with $\epsilon > 0$ and $\sigma > 0$, describes repulsion between spherical particles of "hardness" n separated by a distance R. When $n = \infty$, the particles are hard spheres of diameter σ. Other values of n can be used to describe excluded volume effects in real systems such as powders and colloids (large n), molecular liquids ($n \approx 12$), and liquid alkali metals (small n).[1,2] Theoretical work on inverse power systems has included investigations of the phase behavior,[3−7] the liquid/solid interface,[8] and the fluid.[9−15]

The aim of this paper is to present some new methods for obtaining the thermodynamic equation of state for general inverse power fluids. The equation of state is useful in developing and testing theories of the fluid state and in predicting phase transitions. The approach taken in this paper differs from that of previous work, which is mainly based on perturbation theory,[2,16−20] in that the virial coefficients are used here to obtain the equation of state. This can be done for any hardness n for which the virial coefficients are known. However, there are few published virial coefficients, except for the limiting hard-sphere fluid. Even for the popular $n = 12$ potential, only the first five virial coefficients have been calculated explicitly.[21] This work therefore consists of two parts. The calculation of virial coefficients for a range of different inverse power potentials is described first, followed by initial attempts to combine these data into a general equation of state.

II. Virial Coefficients

For the inverse power potential defined in eq 1, if the reduced pressure is defined as $\bar{P} = P\beta\bar{\sigma}^3$ and the reduced density is $\bar{\rho} = \rho\bar{\sigma}^3$, where P is pressure, ρ is number density, $\beta = (k_B T)^{-1}$, and $\bar{\sigma} = \sigma(\beta\epsilon)^{1/n}$, then $\bar{P}$ is a function of $\bar{\rho}$, but not of temperature, for each hardness n.[22] The virial series for the reduced pressure is

$$\bar{P} = \sum_{m=1} \bar{B}_m \bar{\rho}^m \tag{2}$$

where the reduced virial coefficients $\bar{B}_m = B_m\bar{\sigma}^{3-3m}$ depend on the hardness n, but not on temperature. The first two virial coefficients are $\bar{B}_1 = 1$ and $\bar{B}_2 = (2\pi/3)\Gamma(1 - 3/n)$.

The virial coefficients are calculated from the usual sum of "diagram integrals",[18] in which each diagram represents an integral of a product of Mayer's f-functions over the coordinates of all the particles but one. For higher virial coefficients (large m), close cancellation occurs between the different diagram integrals, and the fractional accuracy in the virial coefficient is therefore much lower than in each of the diagrams separately. Two methods are commonly used to tackle this problem.

Method 1 involves using the geometric properties of the diagrams to reduce the dimensionality of some of the integrals.[23] For example, the fifth virial coefficient is a sum of 10 nine-dimensional integrals, but five of these can be reduced to one-dimensional integrals and two more can be reduced to six-dimensional integrals. The lower-dimensional integrals can be evaluated more accurately, so the uncertainty in the virial coefficient depends only on a few high-dimensional integrals.

Method 2 involves reducing the number of independent sources of error by using the same numerical integration scheme, with the same points and weights, to evaluate all the different integrals. All the separate integrals are therefore combined into an integration of a single function.[24] Cancellation between diagrams with positive and negative values at the same point in multidimensional space is thereby taken into account efficiently, although cancellation still arises between positive and negative values in different regions of space.

These two methods are mutually exclusive, since all integrals treated by the second method must have the same dimensionality. In this work, the virial coefficients up to the fifth are evaluated using method 1, and the sixth and seventh virial coefficients are evaluated using a combination of method 2 for most of the integrals and method 1 for the remainder.

Integrals using method 1 are evaluated in several different ways. First, two sets of geometric variables are tried: $\{r_{12}, r_{13}, r_{23}, (r_{1j}, r_{2j}, r_{3j}, j \geq 4)\}$ and $\{r_{12}, r_3, \cos\theta_3 (r_j, \cos\theta_j, \phi_j, j \geq 4)\}$, where r_{ij} is the distance between the centers of particles i and j, and $(r_j, \cos\theta_j, \phi_j)$ define the position of particle j in spherical polar coordinates relative to the center of mass of all spheres i where $i < j$ and spheres i and j are "connected" by a

10.1021/jp040709i CCC: $30.25
Published on Web 03/17/2005

Mayer *f*-function. For the first set of geometric variables it is also necessary to consider separately the cases where particle j ($j > 4$) is on the same side as particle 4, or not, of the plane defined by particles 1−3. The radial geometric variables r_{ij} and r_i are then transformed to integration variables s_{ij} and s_i. The geometric variables ($\cos\theta$, ϕ) are used as integration variables without transformation. Two sets of integration variables s are tried: $\{s = r^2, r \le 1; s = (n - 2r^{2-n})/(n-2), r > 1\}$ and $\{s = \pi/4 + (1/2)\sin^{-1}[(2r^2 - r_{max}^2 - r_{min}^2)/(r_{max}^2 - r_{min}^2)]\}$, where r_{min} and r_{max} are the limits of the radial variables. These limits are 0 to ∞ for r_{1j} and r_j, for r_{2j} they are obtained from a triangle condition on (r_{12}, r_{1j}, r_{2j}), and for r_{3j} they are obtained from a tetrahedron condition on (r_{12}, r_{13}, r_{23}, r_{1j}, r_{2j}, r_{3j}). The second set of integration variables is only tried for $r_{3j} \rightarrow s_{3j}$. Finally, the multidimensional integral is evaluated using either Monte Carlo or Conroy[25] points, in the variables s_{ij} or (s_j, $\cos\theta_j$, ϕ_j). These methods both enable the standard errors in the integrals to be estimated, and the methods giving the lowest standard errors in a certain amount of computer time are then used again with more integration points, if necessary, to reduce the standard error below some predetermined value. In general it is found that Conroy points are superior to Monte Carlo points, typically by a factor of 5−10 in the standard error, and that the choice of r_{ij} as geometric variables usually works better than spherical polar coordinates.

Integrals using method 2 are evaluated with a linear spanning tree. The geometric variables are r_{12}, r_{23}, $\cos\theta_3$, (r_j, $\cos\theta_j$, ϕ_j, $j \ge 4$) where (r_j, $\cos\theta_j$, ϕ_j) define the position of particle j in spherical polar coordinates relative to particle $j-1$, and $\theta_2 = \phi_2 = \phi_3 = 0$. All diagrams with a factor of $f(r_{12})\, f(r_{23})\, f(r_{34})$ ... can be integrated in this way, so the labeling of points in each diagram is changed to obtain this factor, if possible. The factor of $\Pi_j[f(r_{j-1,j})r_{j-1,j}^2]$ in the integrand is then removed by a change of variables from r to t, where $dt = f(r)r^2\, dr$ and $t = 0$ when $r = 0$. The transformation between r and t is achieved by table lookup and interpolation. Finally, the integral is evaluated using Conroy points in the variables t, $\cos\theta$, and ϕ.

The number of diagrams that do not contain a linear spanning tree, and hence cannot be evaluated using method 2, is 0 of 10 diagrams for B_5, 2 of 56 diagrams for B_6, and 8 of 468 diagrams for B_7. In previous work, these remaining integrals have been calculated using additional spanning trees.[26,27] In fact, all such diagrams can be efficiently treated using method 1, using the same scheme as described above. For B_6, the two integrals are both one-dimensional. For B_7, six of the integrals are one-dimensional and two are six-dimensional. These eight integrals are evaluated in about 1 min of computer time with a Compaq ES40 computer, giving a standard error of about 0.005 in the reduced virial coefficient. This time and error are both negligible compared to using method 2 for the other 460 integrals.

The calculated virial coefficients are listed in Table 1. Each value in the table is typically obtained using at least 100 samples of about 165 million points each. Significant cancellation of errors is achieved through using method 2, as expected. The largest integrals contributing to the seventh virial coefficient $\bar{B}_7$ are more than 1000 times larger in absolute value than $\bar{B}_7$ itself, and the standard error in the calculated seventh virial coefficient is about 10 times smaller than the largest standard errors in the individual integrals, calculated in the same way.

It can be seen that some of the fourth and higher virial coefficients are negative, even though the potential energy function is entirely repulsive; this contradicts a prediction that the virial coefficients for such systems would all be positive.[28] For $n = 12$, the calculated virial coefficients up to the fifth agree with previous results[21] and improve on their precision, and are also close to the estimated[3] values $\bar{B}_6 = 0.80(2)$ and $\bar{B}_7 \approx 0$, based on molecular simulation data. For "hard" potentials with large n, the virial coefficients are positive, at least up to B_7, and the convergence of the virial series can be accelerated; this is investigated further in the next section. For softer potentials, in particular when n is between about 8 and 16, the higher virial coefficients change in sign but are quite small, and simply truncating the virial series can be better than trying to accelerate its convergence.[21] For lower n, the virial series oscillates, and higher virial coefficients are relatively large, especially for $n < 6$. The use of the virial series is probably not the best starting point for such soft potentials.

TABLE 1: Reduced Virial Coefficients $\bar{B}_m$ for the Inverse Power Potential with Hardness n[a]

n	$\bar{B}_3$	$\bar{B}_4$	$\bar{B}_5$	$\bar{B}_6$	$\bar{B}_7$
5	6.62922	−2.18438	1.4702(1)	0.054(26)	−7.1(12)
5.25	6.28878	−0.84594	−0.5009(3)	2.890(29)	−9.2 (11)
5.5	6.00346	0.13898	−1.3886(1)	3.171(22)	−5.83(87)
5.75	5.76085	0.87836	−1.6947(1)	2.640(19)	−3.34(73)
6	5.55200	1.44261	−1.6886(1)	1.907(15)	−1.62(49)
6.25	5.37027	1.87912	−1.5181(1)	1.205(13)	−0.71(45)
6.5	5.21066	2.22062	−1.2664(1)	0.621(12)	0.74(38)
6.75	5.06933	2.49026	−0.9813(1)	0.214(11)	0.87(29)
7	4.94326	2.70474	−0.6886(1)	−0.089(9)	0.71(25)
7.5	4.72790	3.01424	−0.1332(1)	−0.405(8)	0.49(21)
8	4.55060	3.21509	0.3493(1)	−0.439(7)	0.23(19)
8.5	4.40202	3.34589	0.7425(1)	−0.358(7)	−0.01(18)
9	4.27564	3.43024	1.0833(1)	−0.224(6)	−0.01(15)
9.5	4.16682	3.48315	1.3532(1)	−0.036(5)	−0.08(14)
10	4.07214	3.51443	1.5730(1)	0.143(5)	−0.06(14)
11	3.91542	3.53629	1.8980(1)	0.486(4)	−0.18(12)
12	3.79107	3.52751	2.1150(1)	0.776(4)	−0.03(11)
13	3.69005	3.50371	2.2612(1)	0.995(4)	0.14(10)
14	3.60642	3.47295	2.3602(1)	1.177(4)	0.26(11)
15	3.53609	3.43951	2.4272(1)	1.309(3)	0.59(11)
16	3.47615	3.40566	2.4723(1)	1.415(3)	0.62(11)
18	3.37950	3.34100	2.5215(1)	1.565(3)	0.80(10)
20	3.30505	3.28296	2.5391(1)	1.658(3)	0.89(10)
22	3.24599	3.23201	2.5406(1)	1.712(3)	0.98(8)
24	3.19804	3.18751	2.5338(1)	1.752(3)	1.01(9)
28	3.12496	3.11449	2.5095(2)	1.779(3)	1.14(9)
32	3.07195	3.05769	2.4815(1)	1.793(3)	1.18(9)
36	3.03176	3.01255	2.4546(2)	1.790(3)	1.18(9)
40	3.00026	2.97593	2.4301(2)	1.780(3)	1.12(9)
50	2.94499	2.90912	2.3801(1)	1.766(3)	1.14(9)
60	2.90915	2.86408	2.3428(1)	1.745(3)	1.25(9)
80	2.86546	2.80739	2.2926(1)	1.709(3)	1.11(8)
∞[b]	2.74156	2.63622	2.12139(2)	1.564(2)	1.103(6)

[a] Numbers in parentheses give the standard error in the final digit(s). [b] Reference 26.

III. The Equation of State

For hard spheres, the infinite series occurring in the virial expansion of the pressure can be closely approximated by a rational function. In considering whether the use of a rational function to sum the virial series might be useful for softer inverse power potentials, it is helpful to consider first a function that is known to give satisfactory agreement with the equation of state of hard spheres

$$\bar{P} = \sum_{m=1}^{M} b_m \bar{\rho}^m / (1 - \bar{\rho}/\bar{\rho}_c)^2 \qquad (3)$$

The coefficients b_m are obtained from the corresponding reduced virial coefficients. For hard spheres, a reasonable choice of the

parameter $\bar{\rho}_c$ is the reduced density of close-packed spheres, $\sqrt{2}$, since the pressure must diverge as the reduced density increases to this limit. More elaborate rational functions which have been considered for hard spheres[26] also diverge close to this density. However, $\bar{\rho}_c = 6/\pi$, corresponding to complete filling of space, is also commonly used.[29] This originates from using the Percus−Yevick approximation in the pressure equation for hard spheres. In the remainder of this paper, the equation of state defined by the rational function in eq 3, with $\bar{\rho}_c = 6/\pi$ (which is found to give better results than $\bar{\rho}_c = \sqrt{2}$), is called RF1.

For large values of the hardness parameter n, accelerating the convergence of the virial series is important, but for the $n = 12$ potential, the use of a rational function has been found to give worse results than simply truncating the virial series,[21] and the same is likely to be true for smaller n. This is investigated in more detail below. To find an equation of state which works for both large and small n, it may be useful to note that the singularity in the pressure represented by the denominator of the rational function in eq 3 is only physically reasonable for hard spheres. For all other inverse power potentials, there is no upper limit on the reduced density. This justifies using a rational function in which the singularities are moved away from $\bar{\rho} = \bar{\rho}_c$ into the complex plane as n decreases from infinity, that is

$$\bar{P} = \sum_{m=1}^{M} b_m \bar{\rho}^m (1 + \alpha^2)/[(1 - \bar{\rho}/\bar{\rho}_c)^2 + \alpha^2] \qquad (4)$$

Expanding this equation in powers of the density up to $\bar{\rho}^{M+1}$, and comparing it with the virial series, gives $1 + \alpha^2 = (2\bar{B}_M/\bar{\rho}_c - \bar{B}_{M-1}/\bar{\rho}_c^2)/\bar{B}_{M+1}$. If $\bar{\rho}_c = \sqrt{2}$ and $M = 5$, then $\alpha^2 = 0.08$ for hard spheres, and it increases to about 3.3 as n decreases to 10, which is approximately the expected behavior. When $\bar{B}_{M+1}$ decreases, α increases, and the effect of eq 4 is to switch from a rational function resummation of the virial series to a simple truncation. It is interesting that the seventh virial coefficient predicted from eq 4 with $M = 5$, namely, $\bar{B}_7 = (2\bar{B}_6/\bar{\rho}_c - \bar{B}_5/\bar{\rho}_c^2)/(1 + \alpha^2)$, is within the error of the calculations for $n \geq 10$ when $\bar{\rho}_c = \sqrt{2}$; even the sign change of $\bar{B}_7$ near $n = 12$ is predicted correctly. The equation of state defined by the rational function in eq 4, with $\bar{\rho}_c = \sqrt{2}$ (which is found to give better results here than $\bar{\rho}_c = 6/\pi$), is called RF2.

A different equation of state can be obtained using the concept of a density-dependent effective hard sphere diameter,[16] and relating the compressibility factor Z of an inverse power fluid to the compressibility factor $Z_{HS}(x)$ of a fluid of hard spheres with reduced density x and diameter $d\sigma$, where d is the reduced hard sphere diameter, and σ is defined in eq 1. The relationship used is

$$Z(\bar{\rho}) = \bar{P}/\bar{\rho} = Z_{HS}(\bar{\rho}d^3) \qquad (5)$$

Alternatively, the reduced free energy can be used in eq 5 instead of the compressibility factor, giving a different effective diameter, but this makes little difference to the quality of the results.

The effective hard-sphere diameter is then expanded in powers of the density

$$d = \sum_{m=0}^{M} d_m \bar{\rho}^m \qquad (6)$$

and the coefficients d_m are found for each hardness n by substituting eq 6 into eq 5 and expanding in powers of the density up to $\bar{\rho}^{M+2}$. This gives

$$\bar{B}_2 = \bar{B}_{2,HS} d_0^3 \qquad (7)$$

$$\bar{B}_3 = \bar{B}_{3,HS} d_0^6 + 3\bar{B}_{2,HS} d_0^2 d_1 \qquad (8)$$

$$\bar{B}_4 = \bar{B}_{4,HS} d_0^9 + 6\bar{B}_{3,HS} d_0^5 d_1 + 3\bar{B}_{2,HS}(d_0^2 d_2 + d_0 d_1^2) \qquad (9)$$

and similar equations for higher $\bar{B}_m$. From the accurately known hard-sphere virial coefficients, and the calculated virial coefficients for a particular hardness n, the coefficients d_0, d_1, and d_2 are then obtained from eqs 7, 8, and 9, respectively. The equation of state defined by eq 5, with the hard-sphere diameter defined by eqs 6−9, is called EHS.

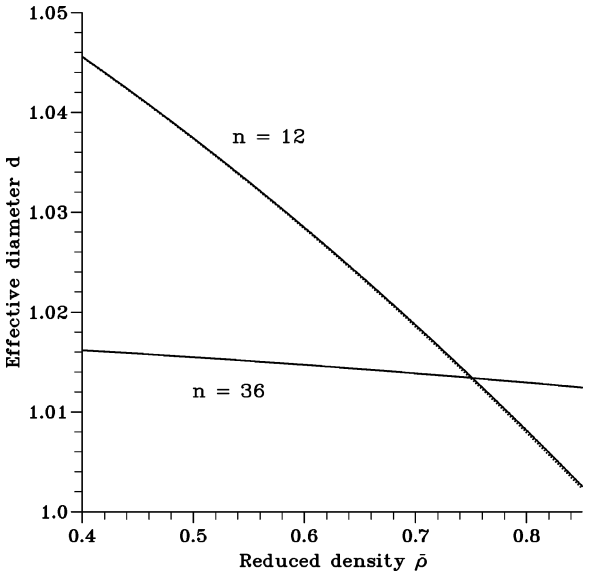

Figure 1. Effective hard sphere diameter d, plotted as a function of reduced density $\bar{\rho}$, for the inverse power potentials $n = 12$ and $n = 36$. The dotted lines are obtained from eqs 6−9, and the solid lines show the result of a fit to d, given in eqs 6, 10, 11, and 12. For $n = 36$, the two lines are indistinguishable.

The effective hard-sphere diameter defined using eq 6 is plotted in Figure 1 for $n = 12$ and $n = 36$, using an expansion in powers of the density up to $M = 2$. Increasing M does not change the diameter greatly. The effective diameter for harder potentials, with larger n, is almost a constant function of the density, whereas the effective diameter for softer potentials, such as the $n = 12$ potential often associated with intermolecular repulsion, decreases rapidly as the density increases.

The RF1, RF2, and EHS equations of state can only be applied to hardnesses n for which virial coefficients have been calculated. To obtain an equation of state which can be used for any hardness, it is necessary to fit or interpolate between the calculated n values. The effective hard-sphere diameter in the EHS equation is a smoother function of n than the virial coefficients and is consequently easier to fit. Using a least-squares method, the following are obtained for $n \geq 10$:

$$d_0 = 1 + 0.57722/n + 2.6366/n^2 + 4.6994/n^3 + 20.4838/n^4 \qquad (10)$$

$$d_1 = -3.9096/n^2 - 18.0600/n^3 - 159.9276/n^4 \qquad (11)$$

$$d_2 = -4.0469/n^2 - 39.3296/n^3 + 220.9507/n^4 \qquad (12)$$

These equations are an extension of the first-order perturbation

TABLE 2: Compressibility Factors for Inverse Power Fluids from Computer Simulation (MD) and Theory[a]

n	$\bar{\rho}$	MD	SUM	RF1	RF2	EHS	FIT
6	0.3984	3.404	3.451	3.445	3.444	3.277	3.067
6	0.5730	5.088	5.211	5.169	5.186	4.472	3.715
12	0.4872	3.696	3.558	3.780	3.773	3.686	3.688
12	0.6685	5.987	5.463	6.412	6.343	5.934	5.940
12	0.7308	7.039	6.277	7.734	7.597	6.947	6.956
12	0.7639	7.666	6.746	8.559	8.364	7.542	7.554
18	0.5164	3.834	3.582	3.862	3.904	3.846	3.846
18	0.6885	6.237	5.320	6.387	6.565	6.323	6.323
18	0.7745	7.988	6.411	8.308	8.639	8.184	8.183
18	0.7818	8.161	6.510	8.497	8.845	8.366	8.365
36	0.5451	3.941	3.594	3.917	3.985	3.944	3.944
36	0.7268	6.724	5.365	6.618	6.938	6.777	6.777
36	0.8176	8.94	6.481	8.733	9.367	9.080	9.079

[a] The equations of state, which use calculated virial coefficients up to the fourth, are defined in the text.

expression $d_0 = 1 + \gamma/n$, $d_1 = d_2 = 0$, where $\gamma \approx 0.57722$ is Euler's constant. The effective hard-sphere diameter defined using these equations is plotted in Figure 1; the fitted diameter almost coincides with the calculated value. The equation of state defined by eqs 5, 6, 10, 11, and 12 is called FIT. It can be used for any inverse power potential and any fluid density, although it is not expected to extrapolate well below $n = 10$.

Table 2 compares "experimental" compressibility factors, calculated using Molecular Dynamics computer simulations,[30] with the predictions of the equations of state RF1, RF2, EHS, and FIT, as defined above, each using the calculated virial coefficients up to $\bar{B}_4$. This means that $M = 4$ for RF1, $M = 3$ for RF2, and $M = 2$ for EHS and FIT. A direct sum of the virial series (eq 2) to $M = 4$ is also used, called SUM. Both EHS and FIT require the hard-sphere compressibility factor $Z_{HS}(x)$, which is approximated by the Carnahan−Starling equation[29]

$$Z_{HS} = \frac{1 + \eta + \eta^2 - \eta^3}{(1 - \eta)^3} \tag{13}$$

where the packing fraction $\eta = \bar{\rho}\pi/6$.

For values of the hardness above $n = 10$, the results show that the EHS equation of state is the closest to the simulation data, and the FIT equation of state is a good approximation to it. The FIT equation of state does not require virial coefficients, so it can be applied to any hardness n, although it should only be used in the fitted range $n \geq 10$. For the $n = 6$ results, the two rational functions RF1 and RF2 perform better than the EHS equation. In all cases, truncating the virial series (SUM) is not the best method for estimating the pressure.

Figures 2 and 3 present data for $n = 12$ and $n = 36$, respectively, obtained with the SUM, RF2, and FIT equations of state, and using calculated virial coefficients up to $\bar{B}_6$ for SUM and $\bar{B}_5$ for RF2. The EHS equation of state using coefficients up to $\bar{B}_4$ is almost identical to the FIT equation of state, so it is not shown in the figures, and it is also found that using higher virial coefficients in the EHS equation of state does not give much improvement. In contrast, the RF2 rational function improves significantly and gives consistently good results, when more than four virial coefficients are used. As expected, truncating the virial series for hardness $n = 12$ at the sixth virial coefficient gives a good representation of the MD simulation results, but this does not apply to the other hardnesses considered.

In conclusion, new calculations of virial coefficients have been carried out for a range of inverse power potentials. These

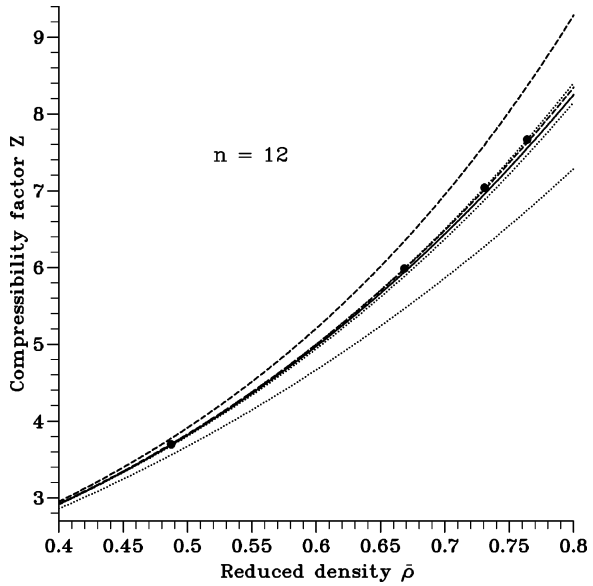

Figure 2. Compressibility factor Z, plotted as a function of reduced density $\bar{\rho}$, for the inverse power potential $n = 12$. Filled circles are results from Molecular Dynamics computer simulation. The solid line is the FIT equation of state, dashed lines are the RF2 equation of state using virial coefficients up to the fourth (upper line) and the fifth (lower line), and dotted lines are obtained by a direct summation of the virial series to the fourth (lowest line), fifth (middle line), and sixth (upper line) virial coefficient.

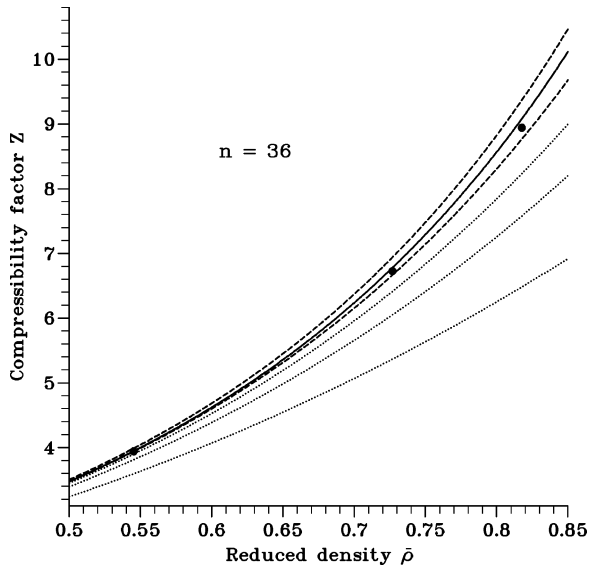

Figure 3. Compressibility factor Z, plotted as a function of reduced density $\bar{\rho}$, for the inverse power potential $n = 36$. Filled circles and lines have the same meaning as in Figure 2.

calculations show that the virial series oscillates for softer potentials, which makes a resummation of the virial series difficult. However, a carefully constructed rational-function resummation appears to give better results than simply truncating the virial series. Calculations of higher virial coefficients can be used to improve the equation of state, but even if only four virial coefficients are known, these can be used (via an effective hard-sphere diameter) to give accurate predictions of the pressure for potentials with hardness $n \geq 10$. On the basis of this observation, a simple fitted equation of state (FIT) is presented, which is expected to be reliable over the same range of hardness.

Acknowledgment. The author is grateful to Professor D. M. Heyes for providing the computer simulation data used in this paper.

References and Notes

(1) Kambayashi, S.; Hiwatari, Y. *Phys. Rev. E* **1994**, *49*, 1251.
(2) Ben-Amotz, D.; Stell, G. *J. Chem. Phys*. **2004**, *120*, 4844.
(3) Cape, J. N.; Woodcock, L. V. *J. Chem. Phys*. **1980**, *72*, 976.
(4) Kol, A.; Laird, B. B. *Mol. Phys*. **1997**, *90*, 951.
(5) Laird, B. B.; Kroll, D. M. *Phys. Rev. A*: *At., Mol., Opt. Phys.* **1990**, *42*, 4810.
(6) Laird, B. B.; Haymet, A. D. J. *Mol. Phys*. **1992**, *75*, 71.
(7) Barrat, J. L.; Hansen, J. P.; Pastore, G.; Waisman, E. M. *J. Chem. Phys.* **1987**, *86*, 6360.
(8) Laird, B. B.; Haymet, A. D. J. *J. Chem. Phys*. **1989**, *91*, 3638.
(9) Heyes, D. M.; Aston, P. J. *J. Chem. Phys.* **1994**, *100*, 2149.
(10) Heyes, D. M. *J. Phys.*: *Condens. Matter* **1994**, *6*, 6409.
(11) Heyes, D. M.; Powles, J. G. *Mol. Phys*. **1998**, *95*, 259.
(12) Powles, J. G.; Heyes, D. M. *Mol. Phys*. **2000**, *98*, 917.
(13) Heyes, D. M.; Powles, J. G. *Mol. Phys*. **2001**, *99*, 1077.
(14) Heyes, D. M.; Powles, J. G.; Rickayzen, G. *Mol. Phys*. **2002**, *100*, 595.
(15) Rickayzen, G.; Powles, J. G.; Heyes, D. M. *J. Chem. Phys*. **2003**, *118*, 11048.
(16) Andersen, H. C.; Weeks, J. D.; Chandler, D. *Phys. Rev. A* **1971**, *4*, 1597.
(17) Verlet, L.; Weis, J.-J. *Phys. Rev. A*: *At., Mol., Opt. Phys.* **1972**, *5*, 939.
(18) Rowlinson, J. S.; Swinton, F. L. *Liquids and Liquid Mixtures*, 3rd ed.; Butterworths: Boston, MA, 1982.
(19) Heyes, D. M. *J. Chem. Phys.* **1997**, *107*, 1963.
(20) Mon, K. K. *J. Chem. Phys.* **2001**, *115*, 4766.
(21) Hoover, W. G.; Ross, M.; Johnson, K. W.; Henderson, D.; Barker, J. A.; Brown, B. C. *J. Chem. Phys*. **1970**, *52*, 4931.
(22) Hansen, J.-P. *Phys. Rev. A*: *At., Mol., Opt. Phys.* **1970**, *2*, 221.
(23) Barker, J. A.; Leonard, P. J.; Pompe, A. *J. Chem. Phys.* **1966**, *44*, 4206.
(24) Ree, F. H.; Hoover, W. G. *J. Chem. Phys*. **1964**, *40*, 939.
(25) Conroy, H. *J. Chem. Phys*. **1967**, *47*, 5307.
(26) van Rensburg, E. J. J. *J. Phys. A*: *At., Mol., Opt. Phys.* **1993**, *26*, 4805.
(27) Vlasov, A. Y.; You, X.-M.; Masters, A. J. *Mol. Phys.* **2002**, *100*, 3133.
(28) Powles, J. G.; Rickayzen, G.; Heyes, D. M. *Proc. R. Soc. London, Ser. A* **1999**, *455*, 3725.
(29) Carnahan, N. F.; Starling, K. E. *J. Chem. Phys*. **1969**, *51*, 635.
(30) Heyes, D. M. Private communication, 2003.